British Journal of Pharmacology (1997) 122, 321–329

Negative chronotropic actions of endothelin-1 on rabbit sinoatrial node pacemaker cells

[1]Hideo Tanaka, Yoshizumi Habuchi, Taku Yamamoto, *Manabu Nishio, *Junichiro Morikawa & Manabu Yoshimura

Department of Laboratory Medicine and *Department of Internal Medicine III, Kyoto Prefectural University of Medicine, Kawaramachi-Hirokoji, Kamigyo-Ku, Kyoto 602, Japan

1 The effects of endothelin-1 (ET-1) on sinoatrial (SA) node preparations of the rabbit heart were studied by means of whole-cell clamp techniques.

2 ET-1 at 1 nM slowed the spontaneous beating activity and rendered half of the cells quiescent. At a higher concentration of 10 nM, the slowing and cessation of spontaneous activity were accompanied by hyperpolarization.

3 In voltage-clamp experiments, ET-1 decreased the basal L-type Ca^{2+} current ($I_{Ca(L)}$) dose-dependently with a half-maximal inhibitory concentration (EC_{50}) of 0.42 nM and maximal inhibitory response (E_{max}) of 49.5%. The delayed rectifying K^+ current (I_K) was also reduced by 33.2 ± 11.1% at 1 nM. In addition, an inwardly rectifying K^+ current was activated by ET-1 at higher concentrations ($EC_{50} = 4.8$ nM). These ET-1-induced changes in membrane currents were abolished by BQ485 (0.3 μM), a highly selective ET_A receptor antagonist.

4 When $I_{Ca(L)}$ was inhibited by ET-1 (1 nM), subsequent application of 10 μM ACh showed no additional decrease in $I_{Ca(L)}$, suggesting the involvement of cyclic AMP in the effects of ET-1 on $I_{Ca(L)}$. In contrast, 1 nM ET-1 further decreased $I_{Ca(L)}$ in the presence of 10 μM ACh, suggesting that ET-1 activates some additional mechanism(s) which inhibit $I_{Ca(L)}$. The ET-1-induced $I_{Ca(L)}$ inhibition was abolished by protein kinase A inhibitory peptide (PKI, 20 μM) or H-89 (5 μM). However, the $I_{Ca(L)}$ inhibition was not affected by methylene blue (10 μM), suggesting a minor role for cyclic GMP in the effect of ET-1 under basal conditions.

5 ET-1 failed to inhibit $I_{Ca(L)}$ when the pipette contained GDPβS (200 μM). However, incubation of the cells with pertussis toxin (PTX, 5 μg ml^{-1}, >6 h) only reduced the ET-1-induced inhibition to 21.5 ± 9.5%, whereas it abolished the inhibitory effect of ACh on $I_{Ca(L)}$.

6 Intracellular perfusion of 8-bromo cyclicAMP (8-Br cyclicAMP, 500 μM) attenuated, but did not abolish the inhibitory effect of ET-1 on $I_{Ca(L)}$. This 8-Br cyclicAMP-resistant component (17.5 ± 14.4%, $n = 20$) was not affected by combined application of 8-Br cyclicAMP with 8-bromo cyclicGMP (500 μM), ryanodine (1 μM) or phorbol-12-myristate-13-acetate (TPA; 50 nM).

7 In summary, ET-1 exerts negative chronotropic effects on the SA node via ET_A-receptors. ET-1 inhibits both $I_{Ca(L)}$ and I_K, and increases background K^+ current. The inhibition of $I_{Ca(L)}$ by ET-1 is mainly due to reduction of the cyclicAMP levels via PTX-sensitive G protein, but some other mechanism(s) also seems to be operative.

Keywords: Endothelin-1; sinoatrial node; chronotropic effect; calcium current; cyclic AMP

Introduction

Endothelin, initially regarded as a potent endogenous vasoconstricting peptide (Yanagisawa *et al*., 1988), has been shown to have various actions on the heart (for review, see Rubanyi & Polokoff, 1993). Due to its potent positive inotropic action, the effects of ET-1 on the L-type Ca^{2+} current ($I_{Ca(L)}$) have been investigated in many studies (Tohse *et al*., 1990; Furukawa *et al*., 1992; Lauer *et al*., 1992; Ono *et al*., 1994; Xie *et al*., 1996). These studies all indicated that endothelin does not affect or slightly (at most by 20%) reduces basal $I_{Ca(L)}$ in myocytes. With regard to the chronotropic action of endothelin, Ishikawa *et al*. (1988) were the first to show that endothelin has a positive chronotropic effect in guinea-pig atria. However, subsequent experimental studies yielded conflicting results, probably depending on the experimental conditions and species used. That is, endothelin was found to either enhance (Ishikawa *et al*., 1991; Ono *et al*., 1995) or reduce (Goetz *et al*., 1988; Karwatowska-Prokopczuk & Wennmalm, 1990; Kim, 1991) the heart rate. Dual (both negative and positive) or no chronotropic effects of endothelin have also been described (Kitayoshi *et al*., 1989; Kurihara *et al*., 1989; Vigne *et al*., 1989; Han *et al*., 1990).

To understand the chronotropic mechanisms of action of endothelin, electrophysiological effects of this peptide on single mammalian pacemaker cells need to be clarified. To date, the chronotropic action of endothelin on single myocytes has been found only in neonatal rat atrial cells by Kim (1991), who demonstrated the negative chronotropic action due to activation of inwardly rectifying muscarinic K^+ channels ($I_{K(ACh)}$). However, no studies on the effect of endothelin on primary pacemaking cells have been published. In guinea-pig atrial cells, Ono *et al*. (1994) demonstrated that endothelin-1 (ET-1) reduces $I_{Ca(L)}$ via inhibition of a adenosine 3′:5′-cyclic monophosphate (cyclicAMP)-dependent pathway in addition to muscarinic K^+ channel activation. These changes, if they occurred in the sino-atrial (SA) node, would result in a decrease in the rate of spontaneous beating. Based on these previous observations, we studied the electrophysiological effects of ET-1 on pacemaker cells isolated from rabbit SA node to address: (1) its chronotropic effects and (2) the underlying ionic mechanisms with special reference to $I_{Ca(L)}$ and the background K^+ current.

[1] Author for correspondence.

Methods

Cell isolation

Isolation of single SA node cells was performed as described previously (Habuchi *et al.*, 1995). The excised hearts from heparin-treated rabbits weighing 2–3 kg (anaesthetised with sodium pentobarbitone at 40 mg kg^{-1} body weight) were perfused, by a Langendorff system, with Ca^{2+}-containing (0.5 mM) phosphate-buffered K^+-containing solution equilibrated with 100% O_2 at 37°C. The composition of the phosphate-buffered solution was as follows (in mM): NaCl 145, KCl 5.4, $MgCl_2$ 1.0, $Na_2HPO_4$2.24, and $CaCl_2$ 1.8 (pH = 7.4, adjusted with NaH_2PO_4 approx. 0.33 mM). After 5 min of perfusion with the Ca^{2+}-containing solution, the perfusate was switched to Ca^{2+}-free solution followed by an enzyme solution containing 10 uml^{-1} collagenase (Yakult, Tokyo, Japan) and 0.08 uml^{-1} protease (Sigma, Type XIV, St. Louis, MO, U.S.A.) for 15 min. A sheet-like preparation (5 × 3 mm) of the SA node was prepared by trimming the surrounding tissue. This was incubated in a second enzyme solution containing 1.3 uml^{-1} type H collagenase (Sigma) and 14 uml^{-1} type III elastase (Sigma) at 37°C. Fifteen to thirty minutes after commencement of the incubation in the enzyme solution (200 μl), aliquots were collected into KB solution containing (in mM) K-glutamate 90, oxalate 10, KCl 25, KH_2PO_4 10, $MgSO_4$ 1, taurine 10, ethylene glycol-*bis* (b-aminoethyl ether)-N,N,N′,N′-tetraacetic acid (EGTA) 0.5, N-2-hydroxyethyl-piperazine-N′-2-ethanesulphonic acid (HEPES) 5 and glucose 10 (pH = 7.2, adjusted with KOH). This procedure was repeated every 3–5 min. After washout of the enzyme from the KB by centrifugation, the cells were stored in KB with 0.1% BSA (Fraction V, Sigma) at 4°C. The cells stored in KB solution were available for 8–12 h for experiments.

Electrical recordings

Spindle-shaped or ovoid SA node cells showing spontaneous beating in the phosphate-buffered solution were used for the experiments. In action potential experiments, clusters composed of 2–5 cells showing well-synchronized activity were used. Spontaneous action potentials were recorded by a perforated-patch method in the phosphate-buffered solution. The pipette was filled with a solution containing (in mM): KCl 144, NaCl 6, HEPES 5 (pH = 7.2, adjusted with HCl). Amphotericin-B dissolved in dimethyl sulphoxide (80 mg ml^{-1}) was added to the solution at a final concentration of 2.4 mg ml^{-1}. Each parameter of the action potentials was defined by averaging ten consecutive action potentials. The overshoot (OS) and the maximal diastolic potential (MDP) were measured from zero potential to the highest and lowest points of the action potential, respectively. The action potential duration (APD_{50}) was measured as the duration at 50% of the action potential amplitude. The maximal upstroke velocity (dV/dt_{max}) was measured as the peak value of the first derivative of the membrane potential digitized at 2 kHz. The amplifier used was an Axopatch 1-D amplifier (Axon Instruments, Foster City, CA, U.S.A.).

$I_{Ca(L)}$ was recorded in two ways. In the perforated-patch method, the amphotericin-B pipette solution with K^+ replaced by Cs^+ was used. The external solution was composed of (in mM):NaCl 140, CsCl 10, HEPES 5, $MgCl_2$ 1.0, $BaCl_2$ 1.0, $CaCl_2$ 1.8 and glucose 10 (pH = 7.4, adjusted with NaOH). $I_{Ca(L)}$ was elicited by 300 ms pulses to 0 mV from a holding potential (HP) of −40 mV every 12 s. In the ruptured-patch method, the pipette-filling solution for the recording of $I_{Ca(L)}$ contained (in mM): Cs-aspartate 85, CsCl 20, $MgCl_2$ 1, HEPES 5, Mg-ATP 5, Na_3-GTP 0.2, Na_2 phosphocreatine 3, EGTA 10, $CaCl_2$ 1 and $MgCl_2$ 1 (pH = 7.2, adjusted with CsOH, pCa was 7.6 according to the stabilizing constants by Fabiato & Fabiato, 1979). A double-pulse protocol was conducted to minimize the rundown of $I_{Ca(L)}$, where a 500 ms prepulse was applied from HP of −80 mV to −40 mV to eliminate the fast Na^+ current and the T-type Ca^{2+} current ($I_{Ca(T)}$). This was followed by 300 ms depolarization to 0 mV to elicit $I_{Ca(L)}$. A liquid-junction potential of 10 mV between the pipette solution and the superfusate was corrected for the ruptured-patch method. $I_{Ca(L)}$ was measured as the difference between the inward peak and the current at the end of the test pulse. In the case of rundown, $I_{Ca(L)}$ change was estimated by comparison between the raw current value during ET-1 application and the estimated value in reference to the time course of rundown under control conditions. Under these K^+-free conditions, the extracellular Cs^+ (10 mM) was supposed to be high to activate the Na^+-K^+ pump and to avoid intracellular Ca^{2+} overload (Eisner & Lederer, 1980). The delayed rectifying K^+ current (I_K) was activated by 300 ms-depolarization to 0 mV. The magnitude of I_K was evaluated from the tail current measured as the difference between the peak of the tail on holding back to −40 mV and the holding current. The hyperpolarization-activated inward current (I_f) was elicited by a 300 ms pulse to −80 mV from HP of −40 mV. In the ramp experiments, the cell was voltage-clamped with the perforated-patch pipette by a ramp pulse from +40 mV to −120 mV over a period of 2 s and repeated every 12 s in the presence of 1 μM nifedipine.

The pipette had a resistance of 1–2 MΩ. The cell capacitance and series resistance were measured from approx. two thirds of the cells tested. The cells had a capacitance of 38.3 ± 7.9 pF (n = 80), and the compensated series resistance measured 6.8 ± 1.3 MΩ for the perforated-patch method (n = 37), and 1.4 ± 0.6 MΩ (n = 43) for the ruptured-patch method. All the experiments were conducted at a bath temperature of 36–37°C.

Chemicals

Endothelin-1 (Peptide Institute, Osaka, Japan) was dissolved in 0.01% acetic acid to make a stock solution of 10 μM. Acetylcholine, isoprenaline (Sigma), and methylene blue (Wako Pure Chemicals, Osaka, Japan) were dissolved in distilled water just before use. BQ485 (perhydroazepin-l-yl-leucyl-D-tryptophanyl-D-tryptophan, Novabiochem, Läufelfingen, Switzerland) and phorbol-12-myristate-13-acetate (TPA, Sigma) were dissolved in dimethyl sulphoxide (500 μM and 1 mM, respectively as stock solutions). Pertussis toxin (PTX), 8-bromo-cyclic 3′,5′-adenosine monophosphate (8-Br cyclicAMP), and 8-bromo-cyclic 3′,5′-guanosine monophosphate (8-Br cyclicGMP) were purchased from Sigma. Guanosine-5′-*O*-(2-thiophosphate) trilithium salt (GDPβs) was from Research Biochemical International (Natick, MA, U.S.A.). Protein kinase A inhibitory peptide (PKI), H-89 (N-[(2-(*p*-bromocinnamylamino)ethyl)]-5-iso-quinoline sulphonamide) and ryanodine were from Calbiochem (La Jolla, CA, U.S.A.).

Data acquisition and statistics

The electrical signals were filtered at 2 kHz in voltage-clamp experiments, but were not filtered in the action potential experiments. They were displayed on a digital oscilloscope (Nicolet 310C, Madison, Wis, U.S.A.) with a sampling rate of 0.01 ms, and the voltage-clamp data were stored on floppy discs. The action potential data were stored on a digital data recorder (TEAC RD101-T, Tokyo, Japan) with a sampling rate of 0.05 ms. The digitised data were analysed on a computer (NEC 98, Tokyo, Japan). The data were expressed as means ± s.d. Statistical analyses were performed by Student's t test, and P values less than 0.05 were considered significant.

Results

Negative chronotropic effects of ET-1

Figure 1a illustrates a typical effect of ET-1 on spontaneous action potentials in SA node cells. ET-1 at 1 nM gradually reduced the action potential amplitude, and subsequently

stopped the beating with little reversal after washout. The corresponding action potentials (triangles) in the lower panel show the reduction of the spontaneous firing frequency (SFF), OS and MDP by ET-1. The dV/dt_{max} was also concomitantly reduced from 7.8 Vs^{-1} to 5.2 Vs^{-1}. Table 1 shows a summary of the action potential parameters before and 1 min after commencement of 1 nM ET-1 application obtained from 10 cell preparations. ET-1 significantly reduced all the parameters measured ($P<0.05$) except APD_{50}. Subsequently five cell preparations stopped beating with a resting potential of -31.3 ± 2.5 mV. At a higher concentration of 10 nM, ET-1 slowed the beating more quickly and hyperpolarization of the MDP developed (Figure 1b). Of eight preparations exposed to 10 nM ET-1, five stopped beating with a resting potential of -65.0 ± 3.1 mV. Little reversal of the action potential waveforms was observed after washout of ET-1 in all the action potential experiments, which did not allow us to carry out repeated experiments on the same preparation.

Changes in the membrane currents by ET-1

To clarify the mechanism(s) underlying the negative chronotropic effects of ET-1, voltage-clamp experiments were conducted on single SA node cells in phosphate-buffered solutions. In Figure 2a, 300 ms depolarizing pulses to 0 mV elicited a peak inward current, and subsequently I_K. In five cells tested, application of 1 nM ET-1 reduced the peak inward current from -465 ± 96 pA to -267 ± 59 pA ($P<0.05$), and the I_K tail from 72.3 ± 43.3 pA to 40.1 ± 23.3 pA ($P<0.05$). The amplitudes of these currents did not recover to the control level following washout of the peptide. Such irreversible or long-lasting effects of ET-1 have also been described for the inotropic (Kelly *et al*., 1990) and chronotropic (Ishikawa *et al*., 1988; Reid *et al*., 1989) effects on the heart. On the other hand, as shown in Figure 2b, ET-1 modified neither the peak inward current nor I_K tail following superfusion of cells with 0.3 μM BQ485 for 5 min, a specific antagonist of ET_A receptors (Itoh *et al*., 1993). Similar results were obtained in all 5 cells tested.

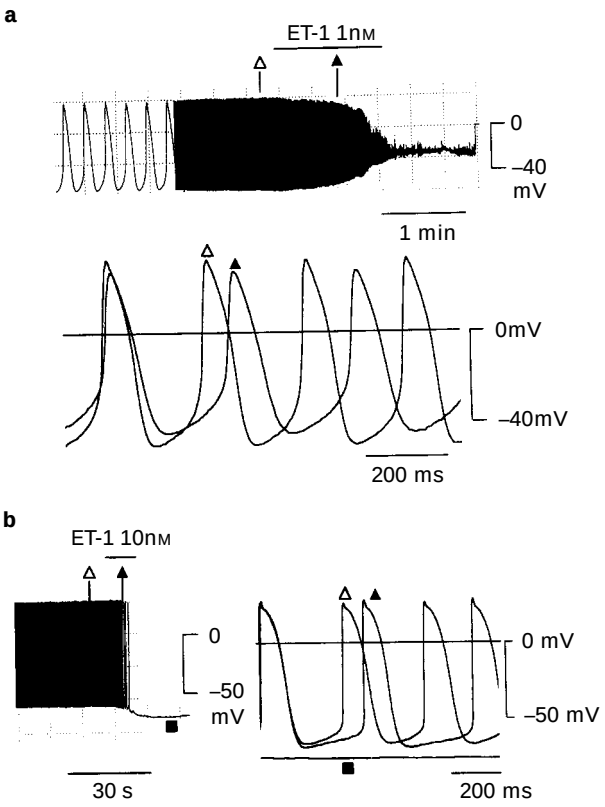

Figure 1 Effects of ET-1 on spontaneous beating action potentials in SA node cell cluster. (a) A low-speed chart recording (upper) and the corresponding action potential waveforms (lower) indicated by symbols. The period of ET-1 (1 nM) superfusion is indicated by the horizontal bar. (b) Hyperpolarization of the spontaneous action potentials and the resting potentials induced by 10 nM ET-1. A low-speed chart recording (left) and the corresponding action potential waveforms (right) indicated by symbols.

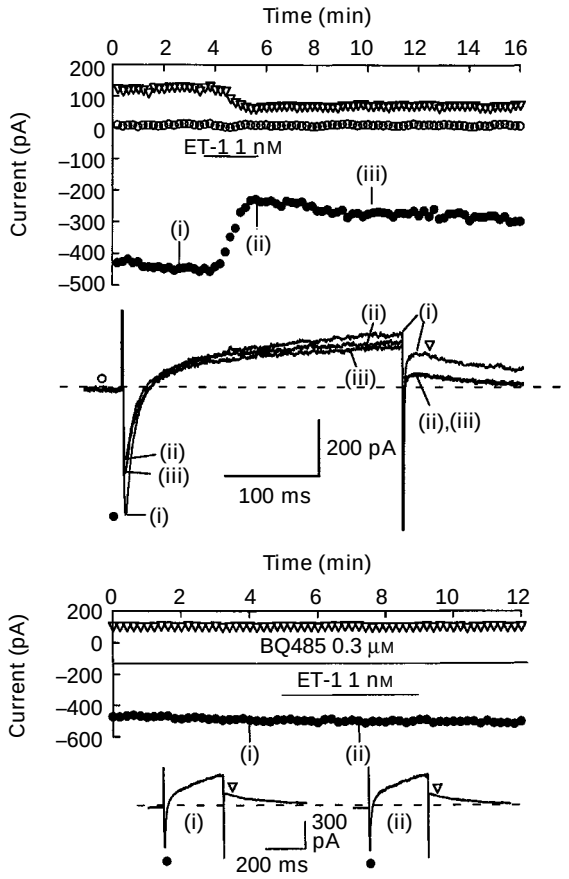

Figure 2 (a) Effects of ET-1 on the membrane currents in a single SA node cell with the perforated-patch method in phosphate-buffered K^+-containing solution. The upper panel illustrates the inward current peak on depolarization, the holding current, and I_K tail on holding back to -40 mV plotted against time. The lower panel shows the corresponding current tracings indicated by numbers (i–iii) in the upper panel. The dotted line in the trace indicates zero current level. (b) Absence of effect of ET-1 on the peak inward current and I_K tail in the presence of BQ485. The current tracings before (i) and during ET-1 (1 nM) application (ii) are shown below.

Table 1 Effects of ET-1 1 nM on the action potential parameters in SA node

	MDP (mV)	*OS* (mV)	dV/dt_{max} (Vs^{-1})	*SFF* (min^{-1})	APD_{50} (ms)
Control	-60.5 ± 4.3	23.9 ± 4.8	8.3 ± 4.1	211 ± 41	81.6 ± 11.3
ET-1	-57.6 ± 4.6*	17.8 ± 7.2*	5.2 ± 2.8*	155 ± 88*	88.8 ± 14.7

Data (means$\pm$s.d. of 10 experiments) were obtained before and 1 min after commencement of ET-1 application. *Denote significance ($P<0.05$) as compared with the control value.

Thus, the membrane current changes induced by ET-1 in SA node cells (Figure 2a) are mediated by ET_A receptors.

The inhibitory effects of ET-1 were more precisely examined on $I_{Ca(L)}$ under K^+ free conditions and on I_K in the presence of nifedipine (Figure 3). ET-1 inhibited $I_{Ca(L)}$ with an EC_{50} of 0.42 nM and E_{max} by 49.5% (solid circles). ET-1 at concentrations of 1 nM or less also inhibited I_K tail (open squares) to a similar extent as the inhibition of $I_{Ca(L)}$. However, activation of a background outward current induced by ET-1 did not allow us to plot a complete dose-response curve for I_K. In line with the hyperpolarization of the membrane potential observed in Figure 1b, this background current developed in response to ET-1 at 3 nM or higher (see below).

Figure 4a shows representative changes in the holding current at -40 mV in response to ET-1 and ACh. The current shifted outward in response to 10 nM ET-1, but not to 1 nM ET-1. The dose-response relationship (Figure 4b, solid circles) revealed that ET-1 activated the holding current with an EC_{50} of 4.8 nM. The current density induced by ET-1 at a saturating concentration (30 nM) was 1.0 ± 0.4 pA pF^{-1}. This value was comparable to that of the I_K tail measured in the experiments in Figure 3 (1.3 ± 0.4 pA pF^{-1}), or that of $I_{K(ACh)}$ activated by 30 nM ACh (open triangles in Figure 4b), indicating that this current was large enough to hyperpolarize the membrane potential. Figure 4c illustrates the current-voltage relationships obtained by the ramp pulse protocol (*see* Methods) before and during superfusion with 10 nM ET-1. The ET-1-induced current showing inward rectification (lower panel) was effectively abolished by subsequent addition of 0.1 mM $BaCl_2$ and was not activated by ET-1 in the presence of 0.3 μM BQ485 ($n=3$, data not shown). The reversal potentials (V_{rev}) for the current (Figure 4d) measured with the ramp experiments showed a slope of 59.1 mV by 10 fold changes in $[K^+]_{out}$ (solid circles), resembling those of $I_{K(ACh)}$ (open triangles). When K^+ in the extracellular and internal perfusate was replaced with Cs^+ by means of the perforated-patch method, ET-1 at 10 nM produced no discernible changes in the background currents (Figure 4e, $n=3$). These findings clearly indicated that the ET-1-induced changes in the background current were the result mostly of an increase in K^+ conductance.

At potentials more negative than -50 mV, I_f is activated in the SA node. Changes in I_f in response to ET-1 may have perturbed the current elicited by the ramp pulses. Indeed, we measured I_f by the perforated-patch method, and found that ET-1 (10 nM) inhibited it to 58.1 ± 35.4% of the control ($n=6$). To test how I_f modified the measurement of V_{rev} for ET-1-induced background current, we measured the reversal potential in the presence of 1 mM CsCl to block I_f. Under these conditions, V_{rev}s for the ET-1-induced current with and without CsCl were similar; -84.7 ± 4.6 mV ($n=3$) vs -82.3 ± 0.6 mV ($n=4$) at 5.4 mM $[K^+]_{out}$, and -99.7 ± 1.5 mV ($n=3$) vs -101.0 ± 1.7 mV ($n=4$) at 2.7 mM $[K^+]_{out}$ respectively, indicating that I_f did not markedly affect measurements of V_{rev}. However, the shape of the current-voltage relationship (lower panel in Figure 4c) may have been somewhat distorted by I_f at negative potentials.

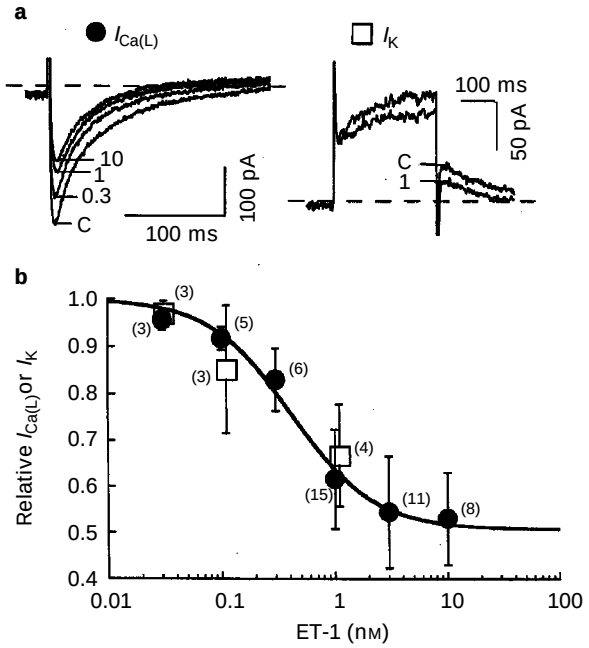

Figure 3 Dose-dependent inhibition of $I_{Ca(L)}$ and I_K by ET-1 by the perforated-patch methods. (a) The left panel shows representative examples of $I_{Ca(L)}$ tracings before (marked as C) and during ET-1 application (0.3, 1 and 10 nM). On the right, I_K tracings with (1) and without (C) 1 nM ET-1 are shown. (b) the relative $I_{Ca(L)}$ and I_K values plotted against concentrations of ET-1. The symbols and vertical lines represent means and s.d., respectively. The smooth curve was drawn according to the least squares fitting of mean values to the equation:

$$\text{relative } I_{Ca(L)} = 1 - E_{max}/(1 + EC_{50}/D)$$

where, D denotes the concentration of ET-1 (nM). The maximal response (E_{max}) = 0.495, half-maximal inhibitory (EC_{50}) = 0.42 nM for $I_{Ca(L)}$. The numbers of experiments are shown in parentheses.

Intracellular mechanisms underlying ET-1-induced inhibition of $I_{Ca(L)}$

Acetylcholine (ACh) inhibits basal $I_{Ca(L)}$ in SA node (Brown & Denyer, 1989; Petit-Jacques *et al.*, 1993) and activates an inwardly rectifying K^+ current ($I_{K(ACh)}$). Taking such similarities in the electrophysiological actions between ET-1 and ACh into account, we tested whether ET-1 inhibits $I_{Ca(L)}$ through the same intracellular mechanisms as ACh. As shown in Figure 5a, when $I_{Ca(L)}$ was inhibited by 1 nM ET-1, further addition of ACh at a saturating concentration of 10 μM (Petit-Jacques *et al.*, 1993) had no effect on $I_{Ca(L)}$; i.e., $I_{Ca(L)}$ was decreased by 42.8 ± 12.0% of the control by 1 nM ET-1, but was not decreased any further by addition of 10 μM ACh ($n=4$). In contrast, when $I_{Ca(L)}$ was maximally inhibited by 40.3 ± 7.9% with 10 μM ACh, subsequent application of 1 nM ET-1 further suppressed it by 22.9 ± 8.8% ($n=4$, Figure 5b).

To examine the intracellular mechanism underlying the ET-1-induced $I_{Ca(L)}$ inhibition the ruptured-patch method was used to modify the intracellular milieu. With this method, 1 nM ET-1 inhibited $I_{Ca(L)}$ by 40.5 ± 9.9% ($n=9$), similar to that obtained with the perforated-patch method. The ACh inhibition of basal $I_{Ca(L)}$ in SA node cells was shown to be mainly due to reduction of the intrinsic cyclic AMP concentration (Petit-Jacques *et al.*, 1993). To assess the roles of cyclic AMP and cyclicAMP-dependent protein kinase (PKA), we examined the effects of ET-1 on cells in which the cyclicAMP-dependent phosphorylation of the Ca^{2+} channels was abolished by PKI (20 μM) in the pipette. The presence of PKI consistently caused a rapid rundown of $I_{Ca(L)}$ to about 20–30% of the initial value 10 min after rupture of the membrane (Figure 5c), suggesting inhibition of the intrinsic phosphorylation of the Ca^{2+} channels in the cells (Petit-Jacques *et al.*, 1993). At 15–20 min after the membrane rupture, isoprenaline (Iso) at 100 nM showed little enhancement of $I_{Ca(L)}$, suggesting sufficient inhibition of PKA activity. Subsequent application of ET-1 at 1 nM showed no inhibition of $I_{Ca(L)}$ ($n=4$). Inclusion in the pipette of H-89 (5 μM), which similarly caused a rapid rundown of $I_{Ca(L)}$ to about 20% of the initial value, also prevented the inhibition of $I_{Ca(L)}$ by 1 nM ET-1 ($n=4$, data not shown). From these observations, it is likely that ET-1 inhibits $I_{Ca(L)}$ only when the Ca^{2+} channels are phosphorylated by PKA.

In addition to PKA, the Ca^{2+} channels are known to be regulated by cyclicGMP (Fischmeister & Hartzell, 1987; Han *et al.*, 1995). This nucleotide, which reduces intracellular cyclicAMP levels via stimulation of the cyclicGMP-stimulated phosphodiesterase (type II PDE) (Méry *et al.*, 1993), was shown to be increased by ET-1 through a PTX-insensitive G

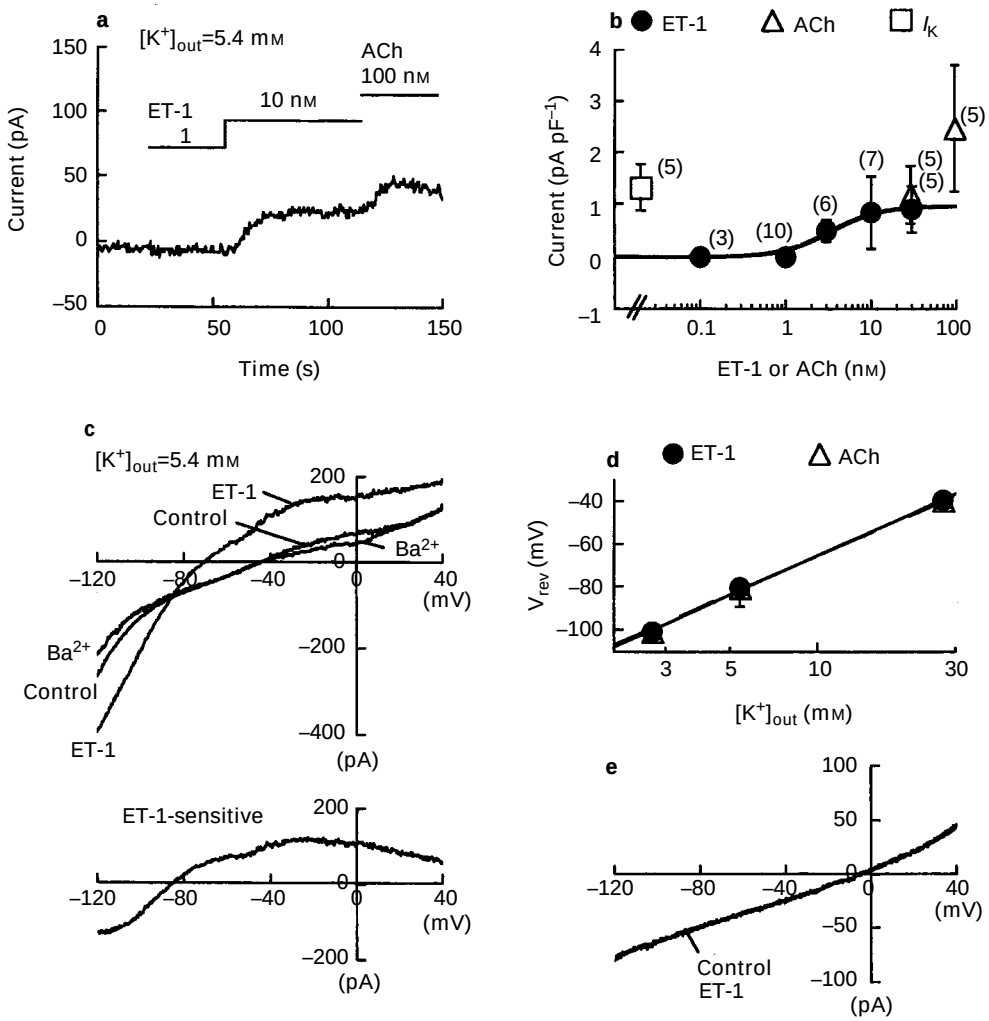

Figure 4 Changes in the background current by ET-1. Cells were superfused with the K^+-containing solution by means of perforated-patch recording with K^+-rich solution. (a) Time course of the holding current at −40 mV by ET-1 and ACh. (b) Dose-response curves for the holding current shift by ET-1 and ACh, and a mean control value of I_K tail. Data are expressed as current densities. The smooth curve was drawn by fitting the mean values to the equation:

$$\Delta I_m = E_{max}/(1 + D/EC_{50})$$

where E_{max} = 1.0 pA pF^{-1}, EC_{50} = 4.8 nM for the holding current changes by ET-1. Each symbol represents the mean value and s.d. The numbers of experiments are shown in parentheses. (c) Current-voltage plots for the background current before and during application of 10 nM ET-1, and subsequent addition of 0.1 mM $BaCl_2$. The cell was voltage-clamped by use of a ramp pulse (see Methods) in K^+-containing solutions with 5 mM HEPES instead of phosphate buffer (pH = 7.4 adjusted with NaOH). The difference currents between with and without 10 nM ET-1 are plotted against voltage in the lower panel. (d) Correlation between $[K^+]_{out}$ and reversal potential (V_{rev}) for ET-1-induced (n = 4) and ACh-induced (n = 3) currents. The straight line was drawn by the least squares fitting. (e) Background current-voltage plots under K^+-free conditions inside and outside the cell.

protein in neonatal rat atrial slices (Shraga-Levine & Sokolovsky, 1996). The possible role of cyclicGMP-related pathways in the ET-1-induced inhibition of basal $I_{Ca(L)}$ was examined with a guanylate cyclase inhibitor, methylene blue (MB). During superfusion with 10 μM MB, ET-1 at 1 nM reduced $I_{Ca(L)}$ by 40.2 ± 9.2% (n = 5), a value similar to that observed without MB. Therefore, it is unlikely that cyclicGMP or type II PDE contributes to the inhibition of basal $I_{Ca(L)}$ by ET-1. The possible role of the cyclicGMP-dependent protein kinase in inhibition of $I_{Ca(L)}$ by ET-1 will be examined further later (see Figure 7b).

The effects of ACh on myocardial membrane currents are characteristically inhibited by PTX, indicating the involvement of a specific G protein. Ono *et al.* (1994) and Xie *et al.* (1996) demonstrated that in guinea-pig myocytes, ET-1 reduces isoprenaline-enhanced $I_{Ca(L)}$ via the PTX-sensitive G-protein. Indeed, the $I_{Ca(L)}$ inhibition by ET-1 in the SA node cells was totally mediated by G-proteins since dialysis with GDPβS (200 μM) completely abolished the effects of ET-1 (Figure 6a, n = 4). However, ET-1 slightly reduced $I_{Ca(L)}$ in the cells treated with PTX (21.5 ± 9.5%, n = 6), despite the observation that the PTX treatment completely prevented the inhibitory effect of ACh in these cells (Figure 6b). In conjunction with the finding that ET-1 inhibited $I_{Ca(L)}$ in the presence of ACh (Figure 5b), this observation indicates that ET-1 has some action(s) in addition to those of ACh.

We next examined the effects of ET-1 on $I_{Ca(L)}$ when the Ca^{2+} channels were fully phosphorylated by PKA dialysis with 8-Br cyclicAMP (500 μM), a non-hydrolyzable cyclicAMP analogue. As shown in Figure 7a, immediately after rupture of the membrane a continuous rundown was observed; i.e. there was no increase in $I_{Ca(L)}$, suggesting that the intracellular 8-Br cyclicAMP concentrations are sufficiently high due to the high concentration of 8-Br cyclicAMP in the pipette (500 μM) and due to the small size of SA node cells. The $I_{Ca(L)}$ amplitude was reduced to 64.2 ± 14.8% of the initial value 5 min after commencement of the recording (n = 20). This time course of rundown was similar to that observed without 8-Br cyclicAMP

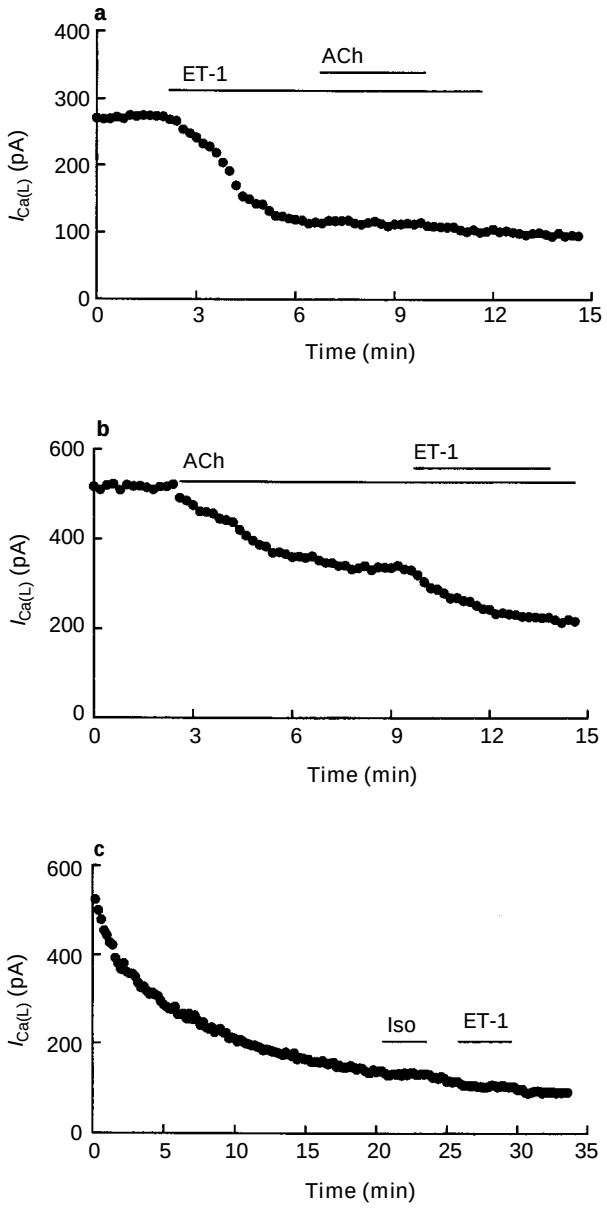

Figure 5 (a) Absence of $I_{Ca(L)}$ inhibition by 10 μM ACh following prior application of ET-1 1 nM. The K^+-free perforated-patch method was used. $I_{Ca(L)}$ was elicited by depolarization to 0 mV from HP of -40 mV. (b) Additional inhibition of $I_{Ca(L)}$ by 1 nM ET-1 after saturating inhibition by 10 μM ACh. Solutions were the same as those used in (a). (c) Absence of $I_{Ca(L)}$ inhibition by isoprenaline (Iso) and ET-1 under intracellular loading with 20 μM PKI. $I_{Ca(L)}$ was recorded immediately after rupture of the membrane.

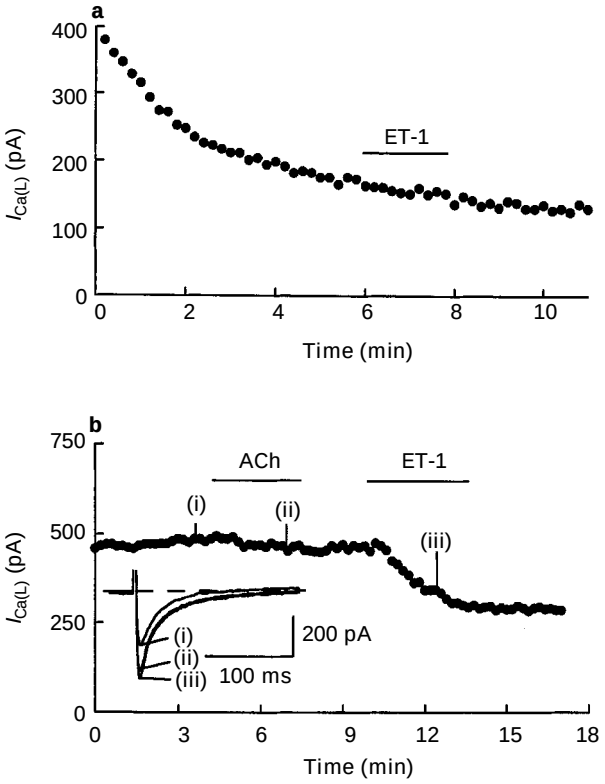

Figure 6 (a) Effects of 1 nM ET-1 on $I_{Ca(L)}$ under internal perfusion with GDPβS (200 μM). A double pulse protocol was used under K^+-free conditions. Rundown of $I_{Ca(L)}$ continued, reaching a quasi-steady state of approx. 35% of the initial value. Note that 1 nM ET-1 failed to inhibit $I_{Ca(L)}$. (b) Effect of ET-1 on $I_{Ca(L)}$ in cells treated with PTX (5 μg ml^{-1}, >6 h). The recordings were made by the perforated-patch method under K^+-free conditions. Note that ACh (10 μM) had no effect on $I_{Ca(L)}$. Further addition of ET-1 (1 nM) inhibited this current by 33%. Inset shows $I_{Ca(L)}$ tracings indicated by arrows on the current plots.

in the pipette (68.9$\pm$12.1% of the initial value after 5 min, $n=7$). Under these conditions, neither isoprenaline (100 nM) nor ACh (10 μM) affected $I_{Ca(L)}$. However, addition of 1 nM ET-1 still inhibited the 8-Br cyclicAMP-stimulated $I_{Ca(L)}$ by 17.5$\pm$14.4% ($n=20$), a value significantly smaller than that observed in the non-dialysed cells (*see* Figure 7c). The 8-Br cyclicAMP-stimulated $I_{Ca(L)}$ was similarly reduced by 1 nM ET-1 even when the cyclicGMP-dependent kinase was fully activated by intracellular loading with 8-Br cyclicGMP (500 μM), i.e. ET-1 at 1 nM reduced $I_{Ca(L)}$ by 16.7$\pm$14.9% in cells loaded with both 8-Br cyclicGMP (500 μM) and 8-Br cyclicAMP (500 μM) ($n=12$).

ET-1 is known to stimulate phosphoinositide hydrolysis by phospholipase C (Vigne *et al.*, 1989). The resultant activation of protein kinase C (PKC) (Hattori *et al.*, 1993) may reduce $I_{Ca(L)}$ (Satoh, 1992). However, prior activation of PKC by TPA (50 nM) did not affect the actions of ET-1 significantly. That is, ET-1 reduced the 8-Br-cyclicAMP-stimulated $I_{Ca(L)}$ by 17.5$\pm$9.7% ($n=6$). The activation of phospholipase C produces inositol triphosphate (IP_3), which mobilizes the Ca^{2+} in intracellular stores. Previously, Tohse *et al.* (1990) demonstrated that ryanodine, an inhibitor of Ca^{2+} release from the sarcoplasmic reticulum, abolished the inhibition of ventricular $I_{Ca(L)}$ by endothelin possibly via Ca^{2+}-induced inactivation. Following pretreatment with ryanodine (incubated in 10 μM ryanodine-containing KB solution for 4 h) plus intracellular dialysis with 10 μM ryanodine and 500 μM 8-Br cyclic AMP, 1 nM ET-1 still reduced $I_{Ca(L)}$ by 19.6$\pm$11.3% ($n=7$). Figure 7c shows a summary of $I_{Ca(L)}$ reduction by ET-1 under various conditions. Briefly, intracellular perfusion with 8-Br cyclicAMP (500 μM) significantly reduced the $I_{Ca(L)}$ inhibition in comparison with the control perfusion (standard solution), and this reduction was not affected by 8-Br cyclicGMP, TPA or ryanodine.

Discussion

Negative chronotropic effects of ET-1

Pacemaker activity in SA node cells is known to be due to a complex interplay of various ionic currents (for review, see Irisawa *et al.*, 1993). Among these currents, $I_{Ca(L)}$ plays a significant role in both the diastolic depolarization and upstroke phase. Deactivation of I_K is also important in diastolic depolarization. I_f and $I_{Ca(T)}$ are operative in early and late phases of the diastolic depolarization, respectively. In addition, small

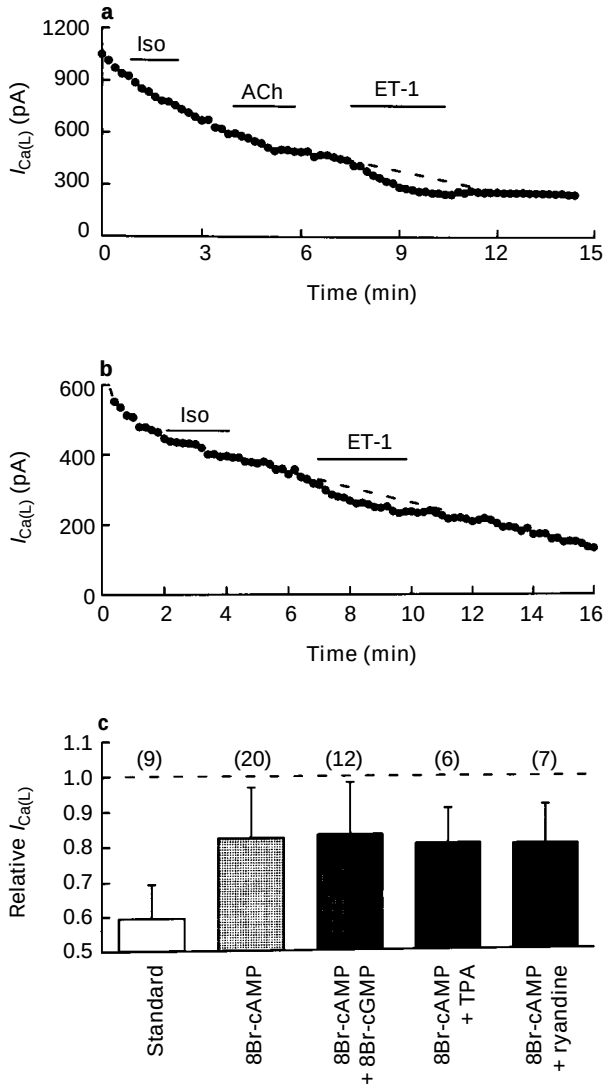

Figure 7 (a) Effects of ET-1 on cells internally loaded with 8-Br cyclicAMP (500 μM). The time course of $I_{Ca(L)}$ rundown was not affected by isoprenaline 100 nM (Iso) or ACh 10 μM. Addition of ET-1 1 nM reduced the amplitude of $I_{Ca(L)}$. The dotted line indicates the extrapolated basal time course of rundown. (b) ET-1 inhibition of $I_{Ca(L)}$ with intracellular perfusion of 8-Br cyclicGMP (500 μM) together with 8-Br cyclicAMP (500 μM). (c) Summary of effects of ET-1 lnM on $I_{Ca(L)}$. Mean current values and s.d. relative to those under control conditions are plotted. Numbers in parentheses denote the numbers of cells examined. *Denotes significance ($P<0.05$) as compared with the value in standard solution.

changes in the time-independent background currents can predominantly affect the electrical activity in SA node. In the present study, we focused on $I_{Ca(L)}$ and the background K^+ current to understand the chronotropic mechanisms of ET-1 in SA node cells because autonomic or hormonal modulations of these currents are important in the control of pacemaking activity (Irisawa *et al*., 1993).

ET-1 exerted potent negative chronotropic effects on SA node cells through ET_A receptors. A gradual slowing of beating with depolarization of MDP was observed at a concentration of 1 nM, whereas 10 nM ET-1 was needed to cause hyperpolarization. These changes suggest that at least two different ionic mechanisms are involved. In the voltage-clamp experiments, 1 nM ET-1 strongly inhibited $I_{Ca(L)}$ (40%) and I_K (33%) (Figure 3b), but the holding current was not modified at this concentration (Figures 2a and 4a). The reduction of dV/dt_{max} and OS should be explained by the inhibition of $I_{Ca(L)}$ and the depolarization of MDP, the inhibition of I_K. Pharmacological inhibition of I_K was shown to suppress the rate of diastolic depolarization on the rabbit SA node (Verheijck *et al*., 1995). Therefore, the attenuation of I_K, in addition to the inhibition in $I_{Ca(L)}$, would also have contributed to slowing of the diastolic depolarization and decrease in SFF. The resting potential induced by 1 nM ET-1 (around -31 mV) was strongly depolarized from the K^+ equilibrium potential. Thus, activation of the background K^+ current seemed to have only a small role in the chronotropic effect of ET-1 at this concentration. On the other hand, ET-1 at 10 nM reduced or completely inhibited the spontaneous beating with hyperpolarization. Similar results were previously obtained in cultured neonatal rat atrial cells by Kim (1991), who suggested that the endothelin-induced negative chronotropic action was exclusively due to the activation of $I_{K(ACh)}$. Other ionic currents may also contribute to the negative chronotropic action of ET-1. ET-1 also inhibited I_f, which must have contributed to slowing of the diastolic depolarization. $I_{Ca(T)}$, which was found to participate in the late phase of the diastolic depolarization (Hagiwara *et al*., 1988), has been shown to be enhanced by ET-1 in neonatal rat myocytes (Furukawa *et al*., 1992). Although we did not examine the effects of ET-1 on $I_{Ca(T)}$ in these pacemaker cells, its enhancement may have attenuated the negative chronotropic effects of ET-1 to some extent. ET-1 has also been shown to enhance the Na^+-Ca^{2+} exchanger (Ballard & Schaffer, 1996). The inward exchange current, if enhanced, would facilitate the diastolic depolarization (Noble, 1984). On the other hand, the attenuation of $I_{Ca(L)}$ by ET-1 in turn would reduce this current during repetitive excitation. Computer simulation studies would be helpful to investigate the roles of these currents in the chronotropic effects of ET-1. In vascular smooth muscle cells, ET-1 induces other background currents such as non-specific cation current (Van Renterghem *et al*., 1988; Chen & Wagoner, 1991) or chloride current (Van Renterghem & Lazdunski, 1993). In the present study, no discernible changes were observed in the background current with ET-1 when K^+ was replaced by Cs^+ (Figure 4e). Therefore, these ET-1-induced background currents are absent, or very small, in the SA node pacemaker cells.

ET-1-induced inhibition of $I_{Ca(L)}$

Our experiments demonstrated that subnanomolar concentrations of ET-1 exhibited a potent inhibitory effect on basal $I_{Ca(L)}$ in SA node. In this tissue, the basal adenylate cyclase activities have been shown to be higher than those in atrial or ventricular myocardium (Taniguchi *et al*., 1979). Potent inhibition by ACh of basal $I_{Ca(L)}$ in SA node cells (Brown & Denyer, 1989; Petit-Jacques *et al*., 1993) has been explained by such a distinctive activity of the intracellular adenylate cyclase, because the inhibitory effects of ACh were abolished when the cells were dialyzed with PKI or cyclicAMP (Petit-Jacques *et al*., 1993). ET-1-induced $I_{Ca(L)}$ inhibition is also likely to be a result of reduction of intracellular cyclicAMP levels, based on the observations that (1) $I_{Ca(L)}$ inhibition by ET-1 was attenuated on cells loaded with PKI (Figure 5c) or 8-Br cyclicAMP (Figure 7a), and (2) the absence of an effect of ACh on $I_{Ca(L)}$ after ET-1 application (Figure 5a). Indeed, ET-1 is known to inhibit cyclicAMP levels enhanced by isoprenaline in rat ventricular myocytes (Hilal-Dandan *et al*., 1992), human atrium (Vogelsang *et al*., 1994) and guinea-pig atrium (Ono *et al*., 1994).

However, ET-1 further reduced $I_{Ca(L)}$ after maximal (i) inhibition by ACh, or (ii) stimulation by 8-Br cyclicAMP, suggesting some additional action(s) of ET-1 to inhibit $I_{Ca(L)}$. Delpech *et al*. (1995) also showed that ET-1 inhibited $I_{Ca(L)}$ in the presence of 8-Br cyclicAMP in guinea-pig atrial cells. We have confirmed that ET-1 inhibited rabbit atrial $I_{Ca(L)}$ during stimulation by isoprenaline, but not under the basal conditions (data not shown). In addition, ET-1 did not inhibit $I_{Ca(L)}$ in SA node cells loaded with PKI (Figure 5c). These observations indicated that ET-1 inhibits $I_{Ca(L)}$ only when the Ca^{2+} channels are phosphorylated by PKA. Such an additional effect of $I_{Ca(L)}$

inhibition was also observed in the effects of ET-1 on the PTX-treated cells (Figure 6b). This observation suggests that ET_A receptors appear to be coupled with some population of G proteins, of which the sensitivity to PTX is different from that of the muscarinic-receptor-linked G_i protein.

There are various possible candidates for the cyclicAMP-resistant inhibitory component of the effect of ET-1 including intracellular Ca^{2+} mobilization (Vigne *et al*., 1989), PKC (Hattori *et al*., 1993), and cyclicGMP (Shraga-Levine & Sokolovsky, 1996), all of which have been shown to mediate the actions of ET-1 on heart cells via PTX-insensitive G protein (Sokolovsky, 1993; Shraga-Levine & Sokolovsky, 1996). However, the present results indicate that none of these mechanisms could explain the 8-Br cyclicAMP-resistant inhibitory component in SA node cells (Figure 7c). ET-1 may affect the phosphorylation-dephosphorylation processes of the Ca^{2+} channels, or ET-1-activated G proteins may affect the channels phosphorylated by PKA.

Changes in the background K^+ currents by ET-1

A small change in the background conductance is sufficient to affect the spontaneous activity of the SA node because of the high membrane resistance (Irisawa *et al*., 1993). In the present study, the ET-1-induced background current was an inwardly rectifying K^+-selective current. Similar current induction in atrial cells by ET-1, with EC_{50} of 20 nM or less, was found by Kim (1991) and Ono *et al*. (1994). In contrast to the stimulating action on these K^+ channels, inhibitory actions of ET-1 on $I_{K(ACh)}$ (Spiers *et al*., 1996) and $I_{K(ATP)}$ (Kobayashi *et al*., 1996) have been observed at concentrations (10–30 nM) similar to those used in the present study. Measurement of the current density at −40 mV revealed that ET-1-induced current was much smaller than that induced by ACh (Figure 4b). The small enhancement of the K^+ conductance by ET-1 may have been due to such a concomitant inhibitory effect of ET-1 on the background K^+ current.

Comparison with previous studies on chronotropic actions of ET-1

The results of the present study are in marked contrast to the previous observations that endothelin increased the beating rate at similar nanomolar concentrations (Ishikawa *et al*., 1988; 1991; Ono *et al*., 1995). An increase in the intracellular Ca^{2+} concentration via ET_B receptors was proposed as the possible mechanisms underlying the positive chronotropic actions in guinea-pig heart (Ono *et al*., 1995). However, the present findings showed that the most consistent action of ET-1 on pacemaker cells was a negative chronotropic effect through ET_A receptors. Considering the observed negative chronotropic action of ET-1 on SA node cells, the different actions in the previous experimental studies may have been explained by some other action(s) of ET-1 on the extranodal tissues. For example, ET-1 releases various vasoactive substances such as atrial natriuretic peptide from the heart (Fukuda *et al*., 1988), prostacyclin and EDRF from the endothelium (De Nucci *et al*., 1988), and noradrenaline from the sympathetic nerve terminals (Sokolovsky *et al*., 1994). Changes in the coronary artery blood flow (Ezra *et al*., 1989; Kurihara *et al*., 1989) are also candidates which may affect the automaticity of the heart. Also, it is important to note that SA node is tonically stimulated by both sympathetic and parasympathetic nervous systems under physiological conditions. Thus, our experimental design, to examine the effects of ET-1 on basal (non-stimulated) electrical activities, would have been different from physiological conditions. The chronotropic actions of ET-1 on SA node *in situ* or under physiological conditions should be a subject for further research.

References

BALLARD, C. & SCHAFFER, S. (1996). Stimulation of the Na^+/Ca^{2+} exchanger by phenylephrine, angiotensin II and endothelin 1. *J. Mol. Cell. Cardiol*., **28,** 11–17.

BROWN, H.F. & DENYER, J.C. (1989). Low-dose acetylcholine reduces calcium current in isolated sino-atrial node cells of rabbit. *J. Physiol*., **410,** 65P.

CHEN, C. & WAGONER, P.K. (1991). Endothelin induces a nonselective cation current in vascular smooth muscle cells. *Circ. Res*., **69,** 447–454.

DELPECH, N., SOUSTRE, H. & POTREAU, D. (1995). Antagonism of β-adrenergic stimulation of L-type Ca^{2+} current by endothelin in guinea-pig atrial cells. *Eur. J. Pharmacol*., **285,** 217–220.

DE NUCCI, G., THOMAS, R., D'ORLEANS-JUSTE, P., ANTUNES, E., WALDER, C., WARNER, T.D. & VANE, J.R. (1988). Pressor effects of circulating endothelin are limited by its removal in the pulmonary circulation and by the release of prostacyclin and endothelium-derived relaxing factor, *Proc. Natl. Acad. Sci. U.S.A*., **85,** 9797–9800.

EISNER, D.A. & LEDERER, W.J. (1980). The relationship between sodium pump activity and twitch tension in cardiac Purkinje fibres. *J. Physiol*, **303,** 475–494.

EZRA, D., GOLDSTEIN, R.E., CZAJA, J.F. & FEUERSTEIN, G.Z. (1989). Lethal ischemia due to intracoronary endothelin in pigs, *Am. J. Physiol*., **257,** H339–H343.

FABIATO, A. & FABIATO, F. (1979). Calculator programs for computing the composition of the solutions containing multiple metals and ligands used for experiments in skinned muscle cells. *J. Physiol. (Paris)*, **75,** 463–505.

FISCHMEISTER, R. & HARTZELL, H.C. (1987). Cyclic guanosine 3′,5′-monophosphate regulates the calcium current in single cells from frog ventricle. *J. Physiol*., **387,** 453–472.

FUKUDA, Y., HIRATA, Y., YOSHIMI, H., KOJIMA, T., KOBAYASHI, Y., YANAGISAWA, M. & MASAKI, T. (1988). Endothelin is a potent secretagogue for atrial natriuretic peptide in cultured rat atrial myocytes. *Biochem. Biophys. Res. Commun*., **155,** 167–172.

FURUKAWA, T., ITO, H., NITTA, J., TSUJINO, M., ADACHI, S., HIROE, M., MARUMO, F., SAWANOBORI, T. & HIRAOKA, M. (1992). Endothelin-1 enhances calcium entry through T-type calcium channels in cultured neonatal rat ventricular myocytes. *Circ. Res*., **71,** 1242–1253.

GOETZ, K.L., WANG, B.C., MADWED, J.B., ZHU, J.L. & LEADLEY, R.J.J.R. (1988). Cardiovascular, renal, and endocrine responses to intravenous endothelin in conscious dogs. *Am. J. Physiol*., **255,** R1064–R1068.

HABUCHI, Y., LU, L.-L., MORIKAWA, J. & YOSHIMURA, M. (1995). Angiotensin II inhibition of L-type Ca^{2+} current in sinoatrial node cells of rabbits. *Am. J. Physiol*., **268,** H1053–H1060.

HAGIWARA, N., IRISAWA, H. & KAMEYAMA, M. (1988). Contribution of two types of calcium currents to the pacemaker potentials of rabbit sinoatrial node cells. *J. Physiol*., **395,** 233–253.

HAN, S-P., KNUEPFER, M.M., TRAPANI, A.J., FOK, K.F. & WESTFALL, T.C. (1990). Cardiac and vascular actions of sarafotoxin S6b and endothelin-1. *Life. Sci*., **46,** 767–775.

HAN, X., SHIMONI, Y. & GILES, W.R. (1995). A cellular mechanism for nitric oxide-mediated cholinergic control of mammalian heart rate. *J. Gen. Physiol*., **106,** 45–65.

HATTORI, Y., NAKAYA, H., NISHIHIRA, J. & KANNO, M. (1993). A dual-component positive inotropic effect of endothelin-1 in guinea pig left atria: a role of protein kinase C. *J. Pharmacol. Exp. Ther*., **266,** 1202–1212.

HILAL-DANDAN, R., URASAWA, K. & BRUNTON, L.L. (1992). Endothelin inhibits adenylate cyclase and stimulates phosphoinositide hydrolysis in adult cardiac myocytes, *J. Biol. Chem*., **267,** 10620–10624.

IRISAWA, H., BROWN, H.F. & GILES, W. (1993). Cardiac pacemaking in the sinoatrial node. *Physiol. Rev*., **73,** 197–227.

ISHIKAWA, T., LI, L., SHINMI, O., KIMURA, S., YANAGISAWA, M., GOTO, K. & MASAKI, T. (1991). Characteristics of binding of endothelin-1 and endothelin-3 to rat hearts. Developmental changes in mechanical responses and receptor subtypes. *Circ. Res*., **69,** 918–926.

ISHIKAWA, T., YANAGISAWA, M., KIMURA, S., GOTO, K. & MASAKI, T. (1988). Positive chronotropic effects of endothelin, a novel endothelium-derived vasoconstrictor peptide. *Pflügers Arch*., **413,** 108–110.

ITOH, S., SASAKI, T., IDE, K., ISHIKAWA, K., NISHIKIBE, M. & YANO, M. (1993). A novel endothelin ET_A receptor antagonist, BQ-485, and its preventive effect on experimental cerebral vasospasm in dogs. *Biochem. Biophys. Res. Commun*., **195,** 969–975.

KARWATOWSKA-PROKOPCZUK, E. & WENNMALM, A. (1990). Effects of endothelin on coronary flow, mechanical performance, oxygen uptake, and formation of purines and on outflow of prostacyclin in the isolated rabbit heart. *Circ. Res*., **66,** 46–54.

KELLY, R.A., EID, H., KRÄMER, B.K., O'NEILL, M., LIANG, B.T., REERS, M. & SMITH, T.W. (1990). Endothelin enhances the contractile responsiveness of adult rat ventricular myocytes to calcium by a pertussis toxin-sensitive pathway. *J. Clin. Invest*., **86,** 1164–1171.

KIM, D. (1991). Endothelin activation of an inwardly rectifying K^+ current in atrial cells. *Circ. Res*., **69,** 250–255.

KITAYOSHI, T., WATANABE, T. & SHIMAMOTO, N. (1989). Cardiovascular effects of endothelin in dogs: positive inotropic action in vivo. *Eur. J. Pharmacol*., **166,** 519–522.

KOBAYASHI, S., NAKAYA, H., TAKIZAWA, T., HARA, Y., KIMURA, S., SAITO, T. & MASUDA, Y. (1996). Endothelin-1 partially inhibits ATP-sensitive K^+ current in guinea pig ventricular cells. *J. Cardiovasc. Pharmacol*., **27,** 12–19.

KURIHARA, H., YAMAOKI, K., NAGAI, R., YOSHIZUMI, M., TAKAKU, F., SATOH, H., INUI, J. & YAZAKI, Y. (1989). Endothelin: a potent vasoconstrictor associated with coronary vasospasm. *Life. Sci*., **44,** 1937–1943.

LAUER, M.R., GUNN, M.D. & CLUSIN, W.T. (1992). Endothelin activates voltage-dependent Ca^{2+} current by a G protein-dependent mechanism in rabbit cardiac myocytes. *J. Physiol*., **448,** 729–747.

MÉRY, P.-F., LOHMANN, S.M., WALTER, U. & FISCHMEISTER, R. (1993). Nitric oxide regulates cardiac Ca^{2+} current: involvement of cGMP-inhibited and cGMP-stimulated phosphodiesterases through guanylyl cyclase activation, *J. Biol. Chem*., **268,** 26286–26295.

NOBLE, D. (1984). The surprising heart; A review of recent progress in cardiac electrophysiology, *J. Physiol*., **353,** 1–50.

ONO, K., ETO, K., SAKAMOTO, A., MASAKI, T., SHIBATA, K., SADA, T., HASHIMOTO, K. & TSUJIMOTO, G. (1995). Negative chronotropic effect of endothelin 1 mediated through ET_A receptors in guinea pig atria. *Circ. Res*., **76,** 284–292.

ONO, K., TSUJIMOTO, G., SAKAMOTO, A., ETO, K., MASAKI, T., OZAKI, Y. & SATAKE, M. (1994). Endothelin-A receptor mediates cardiac inhibition by regulating calcium and potassium currents. *Nature*, **370,** 301–304.

PETIT-JACQUES, J., BOIS, P., BESCOND, J. & LENFANT, J. (1993). Mechanism of muscarinic control of the high-threshold calcium current in rabbit sino-atrial node myocytes. *Pflügers Arch*., **423,** 21–27.

REID, J.J., WONG-DUSTING, H.F. & RAND, M.J. (1989). The effect of endothelin on noradrenergic transmission in rat and guinea-pig atria. *Eur. J. Pharmacol*., **168,** 93–96.

RUBANYI, G.M. & POLOKOFF, M.A. (1993). Endothelins: Molecular biology, biochemistry, pharmacology, physiology, and pathophysiology. *Pharmacol. Rev*., **46,** 325–415.

SATOH, H. (1992). Inhibition in L-type Ca^{2+} channel by stimulation of protein kinase C in isolated guinea pig ventricular cardiomyocytes. *Gen. Pharmacol*., **23,** 1097–1102.

SHRAGA-LEVINE, Z. & SOKOLOVSKY, M. (1996). cGMP formation in rat atrial slices is ligand and endothelin receptor subtype specific. *Circ. Res*., **78,** 424–430.

SOKOLOVSKY, M. (1993). Functional coupling between endothelin receptors and multiple G-proteins in rat heart myocytes. *Recept. Channels*, **1,** 295–304.

SOKOLOVSKY, M., SHRAGA-LEVINE, Z. & GALRON, R. (1994). Ligand-specific stimulation/inhibition of cAMP formation by a novel endothelin receptor subtype. *Biochemistry*, **33,** 11417–11419.

SPIERS, J.P., KELSO, E.J., MCDERMOTT, B.J., SCHOLFIELD, C.N. & SILKE, B. (1996). Endothelin-1 mediated inhibition of the acetylcholine-activated potassium current from rabbit isolated atrial cardiomyocytes. *Br. J. Pharmacol*., **119,** 1427–1437.

TANIGUCHI, T., FUJIWARA, M. & OHSUMI, K. (1977). Possible involvement of cyclic adenosine 3′:5′-monophosphate in the genesis of catecholamine-induced tachycardia in isolated rabbit sinoatrial node. *J. Pharmacol. Exp. Ther*., **201,** 679–688.

TOHSE, N., HATTORI, Y., NAKAYA, H., ENDOU, M. & KANNO, M. (1990). Inability of endothelin to increase Ca^{2+} current in guinea-pig heart cells. *Br. J. Pharmacol*., **99,** 437–438.

VAN RENTERGHEM, C. & LAZDUNSKI, M. (1993). Endothelin and vasopressin activate low conductance chloride channels in aortic smooth muscle cells. *Pflügers Arch*., **425,** 156–163.

VAN RENTERGHEM, C., VIGNE, P., BARHANIN, J., SCHMID-ALLIANA, A., FRELIN, C. & LAZDUNSKI, M. (1988). Molecular mechanism of action of the vasoconstrictor peptide endothelin. *Biochem. Biophys. Res. Commun*., **157,** 977–985.

VERHEIJCK, E.E., VAN GINNEKEN, A.C.G., BOURIER, J. & BOUMAN, L.N. (1995). Effects of delayed rectifier current blockade by E-4031 on impulse generation in single sinoatrial nodal myocytes of the rabbit. *Circ. Res*., **76,** 607–615.

VIGNE, P., LAZDUNSKI, M. & FRELIN, C. (1989). The inotropic effect of endothelin-1 on rat atria involves hydrolysis of phosphatidylinositol. *FEBS Lett*., **249,** 143–146.

VOGELSANG, M., BROEDE-SITZ, A., SCHÄFER, E., ZERKOWSKI, H.-R. & BRODDE, O.-E. (1994). Endothelin ET_A-receptors couple to inositol phosphate formation and inhibition of adenylate cyclase in human right atrium. *J. Cardiovasc. Pharmacol*., **23,** 344–347.

XIE, L.-H., HORIE, M., JAMES, A.F., WATANUKI, M. & SASAYAMA, S. (1996). Endothelin-1 inhibits L-type Ca currents enhanced by isoproterenol in guinea-pig ventricular myocytes. *Pflügers Arch*., **431,** 533–539.

YANAGISAWA, M., KURIHARA, H., KIMURA, S., TOMOBE, Y., KOBAYASHI, M., MITSUI, Y., YAZAKI, Y., GOTO, K. & MASAKI, T. (1988). A novel potent vasoconstrictor peptide produced by vascular endothelial cells. *Nature*, **332,** 411–415.

(Received December 18, 1996
Revised May 27, 1997
Accepted June 11, 1997)